Electrochemical and Solid-State Letters, **10** (1) H23-H26 (2007)
1099-0062/2006/10(1)/H23/4/$20.00 © The Electrochemical Society

Impurities Induced Localized Corrosion Between Copper and Tantalum Nitride during Chemical Mechanical Planarization

Jeng-Yu Lin,[a,z] Yung-Yun Wang,[a] Chi-Chao Wan,[a,*] Hsien-Ping Feng,[a,b] and Min-Yuan Cheng[b]

[a]*Department of Chemical Engineering, National Tsing-Hua University, Hsinchu, Taiwan 300*
[b]*TSMC, Science-Based Industrial Park, Hsinchu, Taiwan 300-77*

Using chemical mechanical planarization, the reaction which causes the formation of localized defects between the interface between the copper (Cu) deposit and the tantalum nitride (TaN) barrier layer were studied. The experimental results of potentiodynamic polarization and secondary ion mass spectroscopy demonstrate that galvanic corrosion was not the dominant factor for such localized defects in our system, most impurities, such as carbon (C) and chloride ion (Cl^-), aggregated near the interface between Cu deposit and TaN barrier layer. As a result, the correlation between localized defects at the Cu/TaN interface and the distribution of impurities is proposed herein.
© 2006 The Electrochemical Society. [DOI: 10.1149/1.2364309] All rights reserved.

Manuscript submitted July 20, 2006; revised manuscript received August 18, 2006. Available electronically November 6, 2006.

Integration of Cu into a semiconductor manufacturing process is implemented with the use of dual damascene approach, in which chemical mechanical planarization (CMP) is employed to remove the protruding Cu deposit and planarize the wafer surface.[1,2] Prior to copper electrodeposition, a thin diffusion barrier layer and a Cu seed layer are deposited onto the features. In particular, Ta and its nitrides have many desirable properties as barrier layer materials and are the primary candidates for copper interconnects.[3-6]

To achieve successful copper metallization, it is important to minimize the copper loss during the CMP process, because the remaining metal line height is directly related to the operation speed of the device and reliability problems.[7] Polished patterned copper wafer with Ta-based barriers while immersed in CMP slurries may induce preferential corrosion of either Cu or barrier material by galvanic corrosion. The literature contains several reports on galvanic corrosion in Cu CMP. Brusic et al.[8] have predicted the likelihood of galvanic corrosion between Ta and Cu immersed in aqueous solutions at different pH values based on polarization data. Tai et al.[9] have also investigated the extent of galvanic corrosion between Cu and four different barrier materials and Ernur et al.[10] have studied the influence of barrier metal types and slurry composition on galvanic corrosion. In addition, Tamilmani et al.[11] measured the corrosion rate between Cu and Ta while both materials were under abrasion by a pad in the presence of peroxide or hydroxylamine-based slurry. So far, they all have focused only on galvanic corrosion between Cu and barrier materials. There is no published information on the correlation between the localized corrosion which occurs at the Cu/TaN interface and the impurity distribution in the Cu deposit which may come from the additives in the plating bath. The packages of additives are usually composed of Cl^-, polyethylene glycol (PEG), bis(3-slfopropyl) disulfide (SPS), and Janus Green B (JGB).[12] The objective of this study was to investigate and build the relation of localized defects at Cu/TaN interface and the distribution of impurities.

Experimental

Sample preparation.— TaN and Cu blanket used in this study were 12 in. Si(100) wafers coated with 30 nm TaN and 30 nm TaN/150 nm Cu seed layers/700 nm Cu electrodeposited layer, respectively, where TaN and Cu seed layers were deposited by physical vapor deposition (PVD) at room temperature without vacuum breaking. Two series of Cu blanket wafers, film A and film B were electroplated with same current density from two different electrochemical plating (ECP) tools, tool A and tool B, which contained different organic additive levels. As for patterned wafers, they were generated by optical lithography and anisotropic etching processes. Here, two series of 12 in. Cu pattern wafers, wafer A and wafer B were also electroplated with same current density from the above different ECP tools, tool A and tool B, respectively. The post-electroplating annealing was performed at 220°C with fixed time

Electrochemical measurements.— The Cu CMP was simulated in a corrosion test cell with specially designed base as the polishing platform, the apparatus is schematically shown in Fig. 1, basically following the design reported by Kuiry et al.[13] The potentiodynamic polarization measurements during polishing were performed in three-electrode cells at room temperature using a computer-controlled CHI-602A potentiostat/galvanostat. A fragment of blanket wafer ($1\ cm^2$) was used as the working electrode along with a Pt counter electrode and a saturated silver/silver chloride electrode (SSCE) reference. The potentiodynamic polarization sweep of the working electrode was performed from −1 (SSCE) to +1 V (SSCE) at 1 mV/s scan rate. The Rodel IC1010 pads were used as the polishing pad for the corrosion experiments herein. The downward force during polishing was measured using a weighing balance supporting the entire electrochemical cell. Here, the downward force used in polarization measurement was around 2 psi. In this configuration, the sample was rotated on the pad under pressure. After the abrasion cell was assembled, the commercial slurry (150 mL) was poured into the vessel. During polishing, the sample was rotated at 200 rpm. In this measurement, alkaline peroxide-based commercial slurries, TA and TB, were employed, respectively. In practice, the pattern wafers were polished in two steps, in which slurry TA was applied in the first polishing step to primarily remove Cu deposits

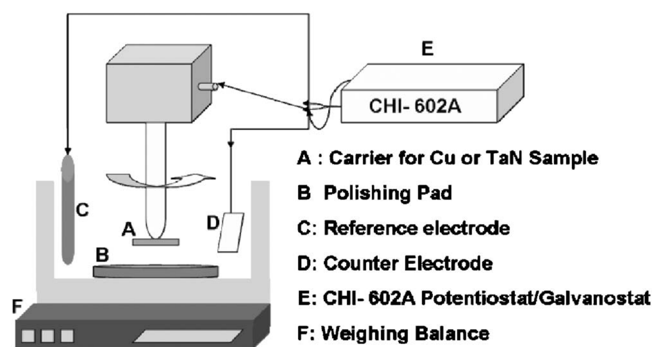

Figure 1. Schematic representation of an apparatus for measuring corrosion behavior.

* Electrochemical Society Active Member.
z E-mail: d923615@oz.nthu.edu.tw

Downloaded on 2015-05-22 to IP 145.94.209.111 address. Redistribution subject to ECS terms of use (see ecsdl.org/site/terms_use) unless CC License in place (see abstract).

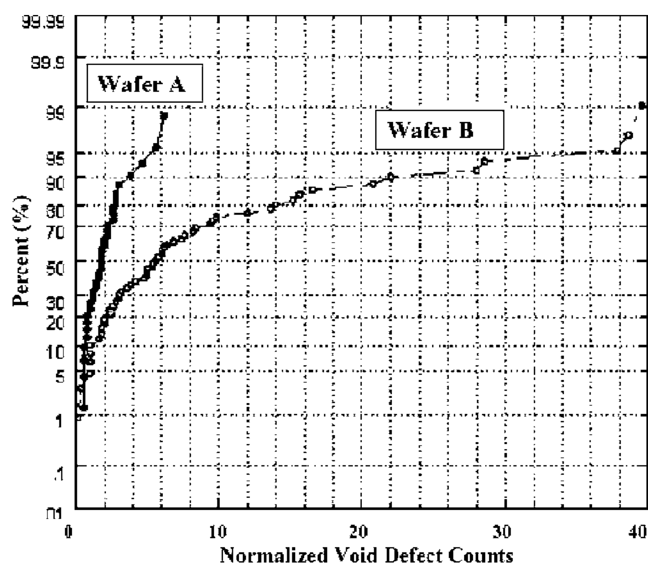

Figure 2. Probability chart of void defects formed on wafer A and wafer B after Cu CMP process.

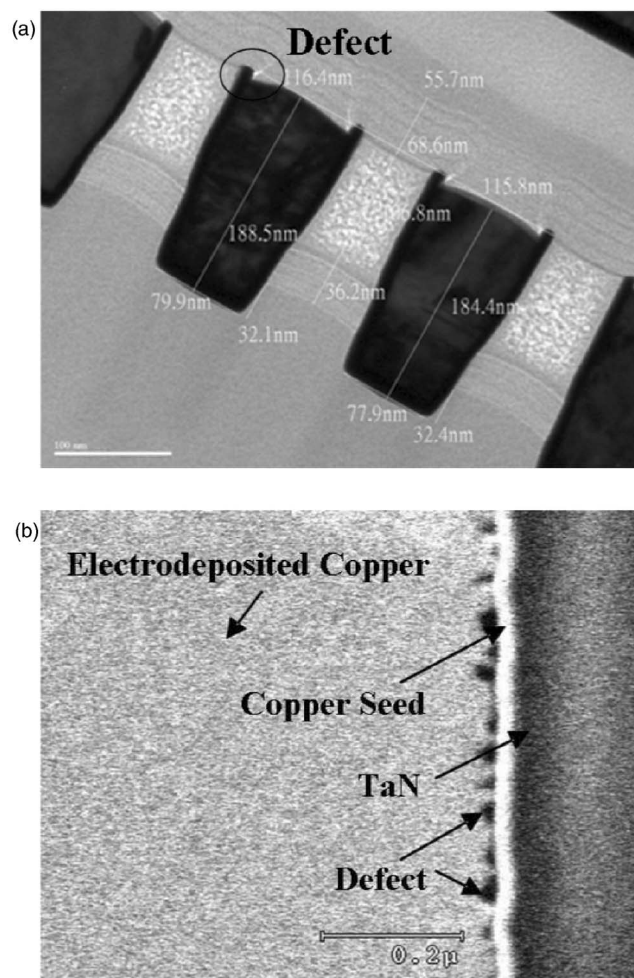

Figure 3. (a) Cross-sectional and (b) top-view images of void defects found at the interface between Cu deposit and TaN layer.

and then slurry TB was used in the second polishing step to removed TaN barrier substantially. In polarization measurements, the Cu blanket wafer used was electroplated by ECP tool B.

Detection of void defects after CMP.— 12 in. pattern wafers were used in this statistical analysis and observation. Pattern wafers with copper electrodeposition were polished with CMP process. The employed down force of CMP was 2 psi; the speeds of polishing head and platen were 90 and 50 rpm, respectively. After Cu CMP process, optical scan method (KLA) was also used to detect types of defects on Cu deposit and to show the topography of void defects by scanning electron microscope (SEM) reviewing system. The cross-sectional images of void defects were detected by transmission electron microscope (TEM) and the samples were prepared with the use of a focused ion beam (FIB).

Investigation of impurity distribution.— Cu blanket wafers, film A and film B, were employed in this analysis. The impurities incorporated in Cu films including carbon and chloride ion were analyzed by CAMECA IMS-6F secondary ion mass spectroscopy (SIMS).

Results and Discussion

To compare the amount of void defects formed on wafer A and wafer B after Cu CMP, statistical technique was employed. The probability of void defects on wafer A and wafer B after CMP are shown in Fig. 2. For instance, at 70% probability, wafer A had around 2 normalized void defect counts while wafer B had about 10. It means that the normalized void defect counts on wafer B were less 10 with 70% probability; however, those on wafer A were less than 2. In other words, the normalized void defect counts on wafer B and on wafer A ranged from 10 to 40 and from 2 to 6 with 30% probability, respectively. It is clear that the void defects induced on wafer B were more than on wafer A after Cu CMP. In particular, most void defects were found on wafer B in this type, as shown in Fig. 3. Figures 3a and b show the cross-sectional and top-view images of void defects on wafer B. Figure 3a demonstrates that the loss of Cu occurred near the opening sides of features on wafer B. Figure 3b shows that the localized defects occurred in the Cu deposit rather than in the TaN.

Galvanic corrosion can occur when two dissimilar materials are coupled in a corrosive electrolyte. Potentiodynamic polarization measurement has been the commonly used technique to simulate the corrosion characteristics of metals during CMP process.[11,13,14] To identify whether such localized defects derived from galvanic corrosion, potentiodynamic polarization curves of Cu film electroplated from tool B and TaN film in commercial slurries used in Cu CMP process were studied and shown in Fig. 4. In particular, all polarization curves were measured under polishing condition. During Cu CMP process, the two-step polishing was employed. To examine whether the galvanic corrosion of Cu deposits occurs during Cu CMP process, the two commercial slurries TA and TB, should be employed in polarization measurements, respectively. The polarization curves show that Cu and TaN are likely to form a galvanic couple, as the anodic branch of TaN polarization curve intersects the cathodic branch of Cu either in slurry TA or in slurry TB. In addition, the galvanic potential and galvanic current density (marked by arrow) can be estimated from the intersectional point of the anodic portion of the TaN curve and the cathodic portion of the Cu portion. The value of galvanic current density measured in slurry TA and TB were around 120 and 100 $\mu A/cm^2$, which were similar to the galvanic current density measured in Cu/Ta system in peroxide-based slurry at pH 8.[11] It was also found that the open-circuit potential (OCP) of TaN was lower compared with that of Cu immersed in TA as well as in TB with abrasion. In a galvanic couple, one of the metals, which is less noble, functions as the anode and the other as cathode. Therefore, in this case TaN and Cu acted as anode and cathode, respectively. It implies that TaN corroded faster than it would have if without Cu. On the other hand, the corrosion of Cu slowed down because of the coupling effect. If galvanic corrosion took place during Cu CMP process, the loss of TaN must be larger than that of Cu. However, Fig. 3 shows the defects on wafer B were

Downloaded on 2015-05-22 to IP 145.94.209.111 address. Redistribution subject to ECS terms of use (see ecsdl.org/site/terms_use) unless CC License in place (see abstract).

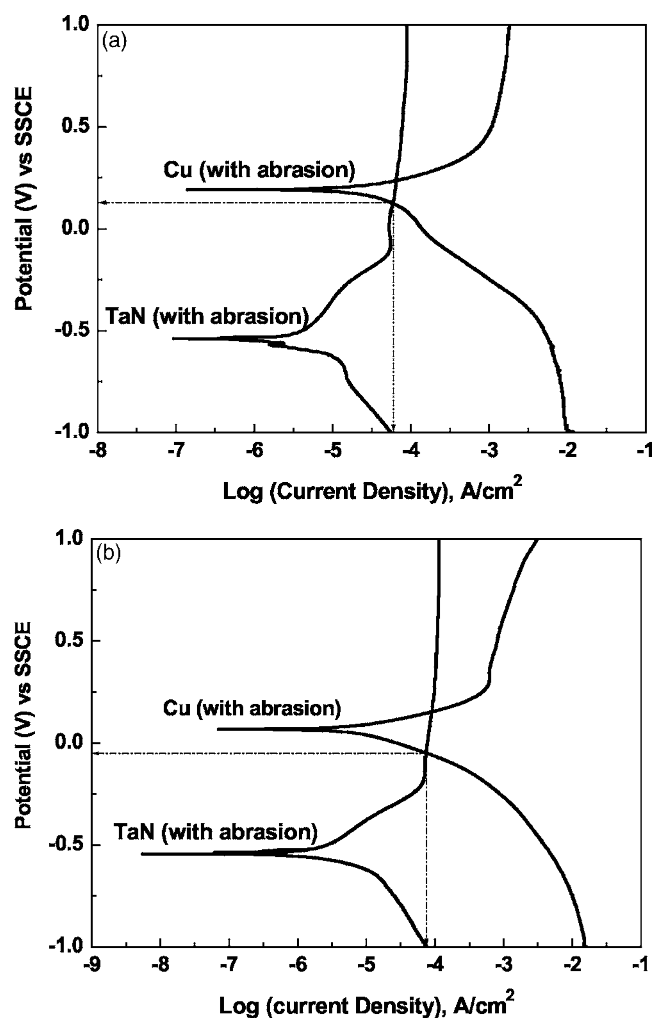

Figure 4. Potentiodynamic polarization of Cu and TaN in commercial slurries. (a) TA and (b) TB.

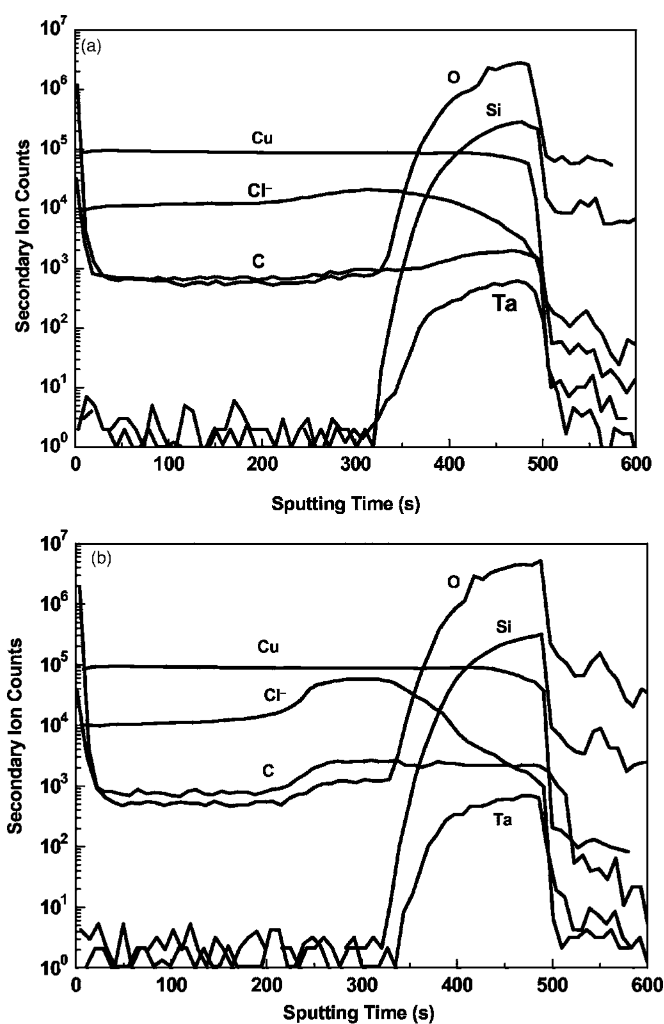

Figure 5. Secondary ion counts for (a) film A and (b) film B plotted against the sputtering time.

located in Cu deposit rather than in TaN barrier layer, which implies the defects on wafer B should result from reaction other than galvanic corrosion.

Figure 5 demonstrates the SIMS depth profiles for the two Cu blanket wafers, called film A and film B, respectively, to identify the incorporation of additives into Cu deposits with two different ECP tools. The Cu/TaN interface in film A and film B was located at sputtering time equal to 325 s due to the increase of Ta element. Apparently, the amount of incorporated Cl^- and C near the Cu/TaN interface in film B is larger than that in film A. Many researchers have detected Cl^-—Cu^+—PEG complexes adsorbed on the surface of Cu deposit, where PEG is a polymer with large molecular weight and the source of C impurity.[15-18] Moreover, several previous studies have utilized SIMS to analyze the formation of Cu complex.[19-21] Zheng et al.[20,21] have found that the impurities, C and Cl^-, derived from Cl^-—Cu^+—PEG complexes are incorporated in the Cu deposit. Hence, we suggest that more Cl^-—Cu^+—PEG complexes adsorbed on the surface of film B than that of film A at the beginning of electrodeposition. Because the more Cl^-—Cu^+—PEG complexes were incorporated near the Cu/TaN interface in film B compared with that in film A, it suggests that the more Cl^-—Cu^+—PEG complexes adsorbed at the beginning of electrodeposition while Cu electroplating was carried out in tool B than in tool A.

As for filling IC features, Cl^-—Cu^+—PEG complexes inhibits deposition on the surface outside the features due to diffusion limitation. Because the more Cl^-—Cu^+—PEG complexes adsorbed at the start of electrodeposition as Cu electroplating was performed in tool B, the incorporation of Cl^-—Cu^+—PEG complexes on the surface outside the features on wafer B electroplated from tool B would be larger than that on wafer A electroplated from tool A. Moreover, Zheng et al.[20,21] further found the incorporation of Cl^-—Cu^+—PEG complexes increased with decreasing line width. As a result, it implies the incorporation of Cl^-—Cu^+—PEG complexes on the surface outside the features on wafer B would be enhanced compared with film B with the same ECP tool B. Therefore, much more Cl^-—Cu^+—PEG complexes would adsorb on the surface outside the features on wafer B.

Several studies have been mentioned that Cu reacts in the presence of H_2O_2 can form a weak passivation layer during Cu CMP process.[22-24] Furthermore, The Cl^-—Cu^+—PEG complexes are the source of impurities C and Cl^-.[20,21] Zhu et al.[25] noted the role of impurities was to obstruct copper oxide grain growth. Grabke et al.[26] demonstrated the nonmetal atoms (N, C, and S) could affect the initial oxidation of metal or alloy. As for IC features, because Cl^-—Cu^+—PEG complexes primarily adsorbed on the surface outside the features, the more accumulation of C element on surface outside the feature compared with center of the feature will deteriorate the passivation ability during Cu CMP process.

Based on the above reasoning, how localized defects form at the interface between Cu deposit and TaN layer is proposed as follows. Initially, the aggregation of C may impede copper oxide grain growth and lead to noncontinuous formation of copper oxide, with

Downloaded on 2015-05-22 to IP 145.94.209.111 address. Redistribution subject to ECS terms of use (see ecsdl.org/site/terms_use) unless CC License in place (see abstract).

less passivation ability. Hence, the surface outside the feature is less passivated. At the same time, aggregation of Cl^- may attract more H^+, leading to an intense localized dissolution of the copper deposits, so-called pitting corrosion. These factors may be why the localized defects take place on the surface outside the features on wafer B easily.

Conclusion

Potentiodynamic polarization curves show that galvanic corrosion is not the cause for localized defects between Cu deposit and TaN during CMP. However, the results from SIMS analysis demonstrated that impurities, such as C and Cl^-, aggregated at the interface between Cu and TaN may result in localized defects at the interface between Cu and TaN. Such impurites may come from the adsorption of Cl^-—Cu^+—PEG complexes on the surface outside the features at the beginning of deposition, as they tend to be adsorbed on the surface outside the feature rather than in the feature interior due to diffusion resistance.

Therefore, we reason such localized defects are related to distribution of the adsorbed C and Cl^- impurities. Carbon impurities tend to aggregate on surfaces outside the feature, rendering less passivation due to the discontinue growth of copper oxides and then the aggregation of Cl^- may attract more H^+, resulting in pitting corrosion.

Acknowledgments

The authors thank the National Science Council of Republic of China, Taiwan, for partially supporting this research under contract no. NSC-94-2214-E-007-005 and NSC-94-2214-E-007-008. Technical supports from Taiwan Semiconductor Manufacturing Company (TSMC) is also appreciated.

National Tsing Hua University assisted in meeting the publication costs of this article.

References

1. P. Singer, *Semicond. Int.*, **6**, 91 (1998).
2. C. Lingk and M. E. Gross, *J. Appl. Phys.*, **84**, 5547 (1998).
3. T. Oku, M. Uekubo, E. Kawakami, K. Nii, T. Nakano, T. Ohta, and M. Murakami, in *Proceedings of the 12th International IEEE VLSI Multilevel Interconnection Conference*, IEEE, p. 182 (1995).
4. S. C. Sun, M. H. Tsai, C. E. Tsai, and H. T. Chiu, in *12th International IEEE VLSI Multilevel Interconnection Conference*, IEEE, p. 157 (1995).
5. E. Kolawa, J. S. Chen, J. S. Reid, P. J. Pokela, and M. A. Nicolet, *J. Appl. Phys.*, **70**, 1369 (1991).
6. K. Holloway, P. M. Fryer, C. Cabral, Jr., J. M. E. Harper, P. J. Bailey, and K. H. Kelleher, *J. Appl. Phys.*, **71**, 5433 (1992).
7. S. Jung, J. Uom, W. Cho, Y. Bae, Y. Chung, K. Kim, and K. Kim, in *Proceedings of the Reliability Physics Symposium 2001*, IEEE, p. 42 (2001).
8. V. Brusic, R. Kistler, S. Wang, J. Hawkins, and C. Schmidt, *Chemical Mechanical Planarization in Integrated Circuit Device Manufacturing*, I. Ali, S. Raghavan and R. L. Opila, PV 98-7, p. 119, The Electrochemical Society Proceedings Series, Pennington, NJ (1998).
9. K. Tai, H. Ohtorii, S. Takahashi, N. Komai, H. Horikoshi, S. Sato, Y. Ohoka, Y. Segawa, M. Ishihara, Z. Yasuda, and T. Nogami, in *Proceedings of the IEEE 2002 Interconnect Technology Conference*, IEEE, p. 194 (2002).
10. D. Ernur, S. Kondo, D. Shamiryan, and K. Maex, *Microelectron. Eng.*, **64**, 117 (2002).
11. S. Tamilmani, W. Huang, and S. Raghavan, *J. Electrochem. Soc.*, **153**, F53 (2006).
12. P. Taephaisitphongse, Y. Cao, and A. C. West, *J. Electrochem. Soc.*, **148**, C492 (2001).
13. S. C. Kuiry, S. Seal, W. Fei, J. Ramsdell, V. H. Desai, Y. Li, S. V. Babu, and B. Wood, *J. Electrochem. Soc.*, **150**, C36 (2003).
14. D. Tamboil, S. Seal, and V. Desal, *J. Vac. Sci. Technol. A*, **17**, 1168 (1999).
15. B. H. Wu, C. C. Wan, and Y. Y. Wang, *J. Appl. Electrochem.*, **33**, 823 (2003).
16. M. Yokoi, S. Konishi and T. Hayashi, *Denki Kagaku oyobi Kogyo Butsuri Kagaku*, **52**, 218 (1984).
17. J. P. Healy and D. Pletcher, *J. Electroanal. Chem.*, **338**, 155 (1992).
18. G. A. Hope and G. M. Brown, in *Electrode Processes VI*, A. Wieckowski and K. Itaya, Editors, PV 96-8, p., 215, The Electrochemical Society Proceedings Series, Pennington, NJ (1996).
19. S. Deshpande, S. C. Kuiry, M. Kliomov, and S. Seal, *Electrochem. Solid-State Lett.*, **8**, G98 (2005).
20. W. Zhang, S. H. Brongersma, N. Heylen, G. Beyer, W. Vandervorst, and K. Maex, *J. Electrochem. Soc.*, **152**, C832 (2005).
21. W. Zhang, S. H. Brongersma, T. Conard, W. Wu, M. Van Hove, W. Vandervorst, and K. Maex, *Electrochem. Solid-State Lett.*, **8**, C95 (2005).
22. G. Xu, H. Liang, J. Zhao, and Y. Li, *J. Electrochem. Soc.*, **151**, G688 (2004).
23. M. Sonmasundrum, K. Kirtikara, and M. Tanticharoen, *Anal. Chim. Acta*, **319**, 59 (1996).
24. V. R. K. Gorantla, K. A. Assiongbon, S. V. Babu, and D. Roy, *J. Electrochem. Soc.*, **152**, G404 (2005).
25. Y. Zhu, K. Mimura, and M. Isshiki, *Oxid. Met.*, **62**, 207 (2004).
26. H. J. Grabke, *Surf. Interface Anal.*, **30**, 112 (2000).

Downloaded on 2015-05-22 to IP 145.94.209.111 address. Redistribution subject to ECS terms of use (see ecsdl.org/site/terms_use) unless CC License in place (see abstract).